*This manuscript was published as formal in*:
***Carbohydrate Polymers*** 157 (**2017**) 493-502
https://dx.doi.org/10.1016/j.carbpol.2016.10.022
https://www.sciencedirect.com/science/article/pii/S0144861716311821

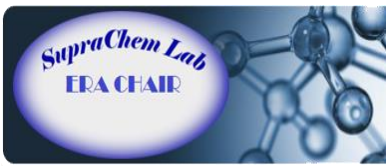


# Title:

# Smart composite materials based on chitosan microspheres embedded in thermosensitive hydrogel for controlled delivery of drugs

Marieta Constantin, Sanda-Maria Bucatariu, Florica Doroftei, Gheorghe Fundueanu*

"Petru Poni" Institute of Macromolecular Chemistry, Aleea Grigore Ghica Voda 41A, 700487, Iasi, Romania

**Running title**: Self-regulated drug delivery systems

***Corresponding author:** Dr. Gheorghe Fundueanu
Department of Natural Polymers, Bioactive and Biocompatible Materials
"Petru Poni" Institute of Macromolecular Chemistry
700487-Iassy, Romania
Tel: +40-232-217454
Fax: +40-232-211299
e-mail: ghefun@icmpp.ro

## Abstract

Smart composite hydrogels (SCHs) consisting of chitosan (CS) microspheres physically embedded within a thermoresponsive hydrogel are synthesized and tested for their capacity of loading and long-term release of a small molecule drug. CS microspheres were used since they display pH-sensitive properties and have the capacity to bind electrostatically the opposite charged salicylic acid (SA), taken as model drug. These microspheres are ulterior physically entrapped within a thermoresponsive hydrogel based on poly(N-isopropylacrylamide-co-hydroxyethylacrylamide) copolymer, cross-linked with N,N'-methylenebisacrylamide. The morphology, swelling behavior, temperature and pH sensitivity, degradability and drug release behavior of the new smart drug delivery system were investigated. Swelling ratios as well as the sharpness of the phase transition, largely depended on the cross-linking degree. The thermoresponsive network slightly protected the CS microspheres from the in vitro degradation. *In vitro* studies showed that the SA followed a prolonged release profile from SCHs in accordance with pH and temperature.

**Highlights**

- A pH/temperature-responsive composite hydrogel was designed and developed

- The sharpness of phase transition largely depended to the cross-linking degree

- The release rate of drug strongly depended to the pH and temperature

- The thermo-responsive network had a weak protection against microspheres degradation

*Keywords*: smart composite hydrogel; thermoresponsive polymer; chitosan; microsphere; drug release

## 1. Introduction

Controlled drug delivery systems have been used to defeat the drawbacks of conventional drug formulations (Bajpai & Sonkusley, 2002; Graham & Mc-Neil, 1984). Even if large progress has been made in the controlled drug delivery area, in some cases (i.e. diabetes and rhythmic heart disorders) the drug has to be delivered in response to signals caused by disease and the necessary amount of drug could be adjusted upon the stimulation of such a signal.

Hydrogels have been used extensively in the development of the smart drug delivery systems (Hoffman, 1997). They are composed of three-dimensional network of hydrophilic polymer chains that could be cross-linked by covalent bonds, hydrogen bonding, van der Walls interactions or physical entanglements (Kamath & Park, 1993; Park, Skalaby & Park, 1993). Hydrogels can entrap and protect the drug from hostile environments for the subsequent slow release by diffusion or erosion depending on their state of hydratation. They can also control drug release rate by changing the structure in response to environmental stimuli such as temperature, pH, electric and magnetic fields, solvent composition, light, ions, etc (Amin, Rajabnezhad & Kohli, 2009; Bae, 1997; Hoffman, 1997). These stimuli-sensitive materials are also called “intelligent” or “smart” hydrogels (Park & Park, 1999).

Temperature-sensitive hydrogels have been studied more extensively since the triggering agents for controlled drug release are the changes in temperature (Bromberg & Ron, 1998; Fundueanu et al., 2005). The most popular thermosensitive hydrogel is that based on poly(N-isopropylacrylamide) (PNIPAAm). This hydrogel possess a transition temperature at about 33 $^{o}$C (Bae, Okano & Kim, 1990; Grinberg et al., 2000; Inomata, Wada, Yagi, Goto & Saito, 1995) accompanied by a rapid decrease in the volume of the gel resulting in a fast release of entrapped drug and solvent (Gandhi, Paul, Sen & Sen, 2015). However, it was found that the drug loaded within the PNIPAAm-based hydrogels is quickly released due to the swollen and porous PNIPAAm network (Bae, Okano, Hsu & Kim, 1987; Hoffman, Afrassiabi & Dong, 2015; Zhang, Wu & Chu, 2004; Zhang, Zhuo, Cui & Zhang, 2002).

Recently, smart drug delivery systems obtained by the incorporation of drug-loaded microspheres within the sensitive hydrogel have proved to accomplish the long-term drug delivery. The literature presents several reports concerning smart composite materials such as those based on PLGA microspheres or nanoparticles dispersed in chitosan/PVA hydrogel (Tang, Zhao, Li & Du, 2010), thermoresponsive chitosan/β-glycerophosphate hydrogel (Joung, Choi, Park & Park, 2007), thermoresponsive methylcellulose hydrogel (Lin, Sun, Jiang, Zan & Ding, 2007), etc. In addition, drugs, peptides or growth factors-loaded CS microspheres were incorporated in poly(lactic acid) scaffolds (Niu, Feng, Wang, Guo & Zheng, 2009), mucoadhesive hydrogel (El-Leithy, Shaker, Ghorab & Abdel-Rashid, 2010), or in biodegradable CS scaffolds (Cai et al., 2007; Liu et al., 2012) for the same purpose. Of note, CS is frequently used for the construction of smart composite materials, both as continuous polymeric matrix for the incorporation of different kinds of particles and as microspheres to be embedded in various polymeric matrix. Indeed, CS with excellent biodegradable and biocompatible characteristics, is a naturally occurring polysaccharide which has been extensively applied in the pharmaceutical industry for its potential in the development of drug delivery systems (Illum, 1998; Morris, Kök, Harding & Adams, 2010). In addition, due to the primary amino groups with a pKa of around 6.5, CS is recognized as a natural polymer with pH-sensitive properties.

In this work, we designed and synthesized a temperature- and pH-sensitive drug delivery system by incorporation of CS-based microspheres into poly(N-isopropylacrylamide-co-hydroxyethylacrylamide) (P(NIPAAm-co-HEAAm)) hydrogel. CS microspheres were obtained by suspension crosslinking technique. Salicylic acid, taken as model anionic drug, was loaded into CS microspheres after their physically incorporation into hydrogels. The smart properties of the new drug delivery system were investigated by analyzing the swelling ratio and response kinetics upon cooling and heating. The protective effect of the thermoresponsive network on the *in vitro* degradation of incorporated CS microspheres was studied. The release profiles showed a pattern according to pH and temperature.

## 2. Materials and methods

### *2.1. Materials*

Low molecular weight chitosan (Mw = 104 KDa, DD= 83.5%) (CS), hydroxyethylacrylamide (HEAAm), and salicylic acid (SA) were purchased from Sigma-Aldrich Chemical Co. (St. Louis, USA). N-isopropylacrylamide (NIPAAm), supplied from Sigma-Aldrich Chemical Co. (Milwaukee, WI, USA), was re-crystallized from hexane. Ammonium persulfate (APS), N,N'-methylenebisacrylamide (BisAAm), N,N,N',N'-tetramethylethylenediamine (TEMED) were supplied from Fluka AG (Buchs, Switzerland).

Glutaraldehyde (GA) (aqueous solution 25 %, w/v) was supplied by Fluka AG (Seelze, Germany). Cellulose acetate butyrate (CAB) was purchased from Eastman Inc. (Kingsport, Tennesse, USA). Dichloroethane (DCE) supplied from Chemical Company SA (Iasi, Romania) was used as received.

### *2.2. Methods*

#### *2.2.1. Preparation of chitosan microspheres*

CS microspheres were prepared by the suspension cross-linking procedure. In a 500 mL reactor fitted with a mechanical stirrer, condenser, and thermometer, CS (1 g) was dissolved in 50 mL of an aqueous acetic acid solution (1 %, v/v) and then dispersed in 100 mL of DCE containing 2.4 g CAB (as a stabilizer for suspension). This mixture was stirred at 1000 rpm for 1 hour at 50 $^{o}$C, then 1 mL of GA was added, afterwards the cross-linking reaction continued for another 2 hours. Finally, the chitosan microspheres were recovered by filtration, successively washed with DCE, acetone, water, and acetone and dried in vacuum at 50 °C.

#### *2.2.2. Preparation of smart composite material*

0.85 g of a mixture of NIPAAm and HEAAm (9.5:2 molar ratio) were dissolved in 10 mL distilled water. After complete dissolution of monomers, various amounts of cross-linker (BisAAm) and CS microspheres were added and the mixture was left at room temperature for 2 days for a complete

swelling of microspheres in the above solution. Dried nitrogen was bubbled through the solution for 50 min. Then, the initiator (APS) (3 %, w/w, relative to monomers) and the accelerator (50 µl of TEMED) were added and the mixture was quickly transferred into a syringe (i.d.× h = 15×70 mm). After 24 hours of polymerization, smart composite hydrogels ($SCH_x$; x means the percentage of BisAAm relative to monomers) were obtained. The resulting material was removed from the syringe and kept for 2 days in a large amount of water, frequently refreshed to remove the soluble fraction of polymer and initiator residues. All SCH samples were cut into cylinder-like pieces approximately 15 mm in diameter and 10 mm in thickness for the following studies. Finally, the hydrogel was recovered by drying at room temperature or by lyophilization for further investigations. The feed composition and the preparation conditions of SCH are summarized in Table 1.

Similar preparation conditions were used for the smart hydrogels $SH_x$, without CS microspheres.

### *2.2.3. Morphological and dimensional analysis*

The optical images of the SH and SCH samples were recorded by a Cannon digital camera. CS microsphere size was determined by measuring the diameters of at least 100 microspheres on scanning electron micrographs. The SHs and SCHs swollen in deionized water at room temperature (23 ºC) were quickly frozen in liquid nitrogen and then freeze-dried (-57 °C, $5.5 \times 10^{-4}$ mbar) for at least 24 h until all the solvent was sublimed. The freeze-dried hydrogel was carefully fractured and the interior morphology was observed by an Environmental Scanning Electron Microscope (ESEM), type Quanta 200, operating with secondary electrons in Low Vacuum, at 20 kV.

### *2.2.4. Temperature and pH responsive properties*

#### *2.2.4.1. The equilibrium swelling ratios*

SHs and SCHs swelling ratio was measured at different temperatures ranging from 23 to 60 ºC, controlled up to 0.2 ºC, using a thermostated water bath. Pre-weighed samples were equilibrated in

simulated physiological fluids (standard acidic solution (pH 1.2, 64 mM HCl + 50 mM KCl), standard phosphate buffer (pH 7.4, 50 mM $Na_2HPO_4$ + NaOH)) for at least 24 h at each predetermined temperature. Then, the samples were taken out from the water bath, excess liquid was wiped off from the surface with moistened filter paper, and were weighed. The swelling ratio was determined according to the following equation (1) (Ngah, Endud & Mayanar, 2002).

$$\text{Swelling ratio} = \frac{W_s - W_d}{W_d} \quad (1)$$

Where $W_s$ is the weight of the swollen hydrogel at equilibrium at each temperature and $W_d$ is the weight of the dry weight sample.

The volume phase transition temperature (VPTT) of the hydrogel was determined as the inflexion point of the curve swelling ratio *vs* temperature by Boltzman fitting of the experimental data.

#### *2.2.4.2. Swelling kinetics*

The swelling kinetics of SCHs were studied by immersing dried samples in buffer solutions of pH 1.2 or 7.4, at 23 $^oC$ or 37 $^oC$. The hydrogels were removed from medium at regular time intervals, wiped off with moistened filter paper and then weighed.

#### *2.2.4.3. Swelling/deswelling kinetics*

The oscillatory swelling behavior of SCHs was measured in buffer solutions of pH 1.2 or 7.4 maintained for 2 hours at alternate temperatures of 23 and 42 $^oC$. The SCHs were first equilibrated in buffer solutions at 23 $^oC$, and then quickly transferred at 42 $^oC$. At specified time intervals, the hydrogels were taken out from the medium and weighed as above. The swelling-deswelling behavior was evaluated in terms of swelling ratio which was calculated with equation (1).

### *2.2.5. In vitro degradation study*

The biodegradation study of SCHs (~0.150 g SCH containing ~20 mg CS microspheres) and control CS microspheres (20 mg) was carried out *in vitro* by incubating in 10 mL of PBS (pH 7.4) without or with 1 mg/mL lysozyme, at 37 ºC. 1 mL of the PBS with lysozyme was replaced every 3 days. At predetermined time intervals over 4 weeks, hydrogels and microspheres were taken from the medium, washed with distilled water and freeze-dried. The dry weight remaining ratio was calculated according to the equation (2):

$$\text{Weight remaining } (\%) = \frac{W_t}{W_0} \times 100 \quad (2)$$

Where $W_0$ denotes the initial weight and $W_t$ is the weight at time t.

### *2.2.6. Drug loading and drug release experiments*

For loading SA, each dried hydrogel piece (~ 0.150 g) was soaked in 10 mL of drug aqueous solution (1.5 mg/mL), and maintained immersed for seven days at 22 ºC. Then, the SA-loaded hydrogel was removed, washed with distilled water and the amount of SA remained in the collected solutions was determined by the UV measurements at $\lambda$=295 nm using a previously made calibration curve. The amount of SA loaded in each hydrogel was determined according to the equation (3):

$$SA_{\text{loaded}} = [SA]_i - [SA]_f \quad (3)$$

Where $[SA]_i$ and $[SA]_f$ are the SA concentration in the solution before and after the loading process. The efficiency of drug loading was calculated according to the equation (4):

$$\text{Efficiency } (\%) = \frac{SA_a}{SA_t} \times 100 \quad (4)$$

Where $SA_a$ is the actual amount of drug loaded in hydrogel and $SA_t$ is the theoretical amount of loaded SA.

The theoretical amount is calculated taking into account the CS microspheres content of hydrogel assuming that each amine group of CS microspheres binds electrostatically a SA molecule.

The SA release studies were performed by immersing SA loaded SCHs (about 0.180 g containing cca 5 mg of SA) in standard acidic solution (pH 1.2) or PBS (pH 7.4), at 23, 37, or 42 $^{o}$C. At predetermined time intervals, 3.0 mL of the release solution was taken out and the SA concentration was determined spectrophotometrically at 295 nm, using a previously made calibration curve. The same volume of fresh release medium was added to keep unchanged the volume of release system. To evaluate the effect of temperature cycling on SA release, the SA-loaded SCHs were subjected to thermal cycling, alternating temperatures from 23 $^{o}$C (below the VPTT) to 42 $^{o}$C (above the VPTT). Each thermal cycle comprised of 30 min. At predetermined time interval, 3 mL of release medium was collected and replaced with fresh buffer. The samples were spectrophotometrically analyzed for SA content using a previously made calibration curve.

#### *2.2.7. Statistical analysis*

All data are the result of three independent measurements. The values are presented as mean ± standard deviations.

## 3. Results and discussion

### *3.1. Preparation of CS microspheres*

The CS was chosen as starting material for the synthesis of polymeric microspheres, since it displays advantageous biomedical properties. Indeed, CS is well known as a biodegradable and biocompatible polymer (Illum, Jabbal-Gill, Hinchcliffe, Fisher & Davis, 2001; Majeti & Ravi, 2000) with many biomedical applications in the form of a solution, film, and microspheres (Dash, Federica, Ottenbrite & Chiellini, 2011; Mengatto, Helbling & Luna, 2012; Mitra & Dey, 2011). The CS microspheres were prepared by cross-linking with GA of the polymer aqueous solution dispersed in DCE. The obtained microspheres were light yellow colored. The shape and surface morphology of CS microspheres were investigated using scanning electron microscopy (SEM). The

photographs showed that the microspheres were spherical in shape with folded surface and with a mean diameter in the dried state of 48.8 ± 6 μm (Fig. 1A,B). The exchange capacity of CS microspheres, determined by conductometric titration method (De Alvarenga, de Oliveira & Bellato, 2010), was found to be 3.7 meq/g.

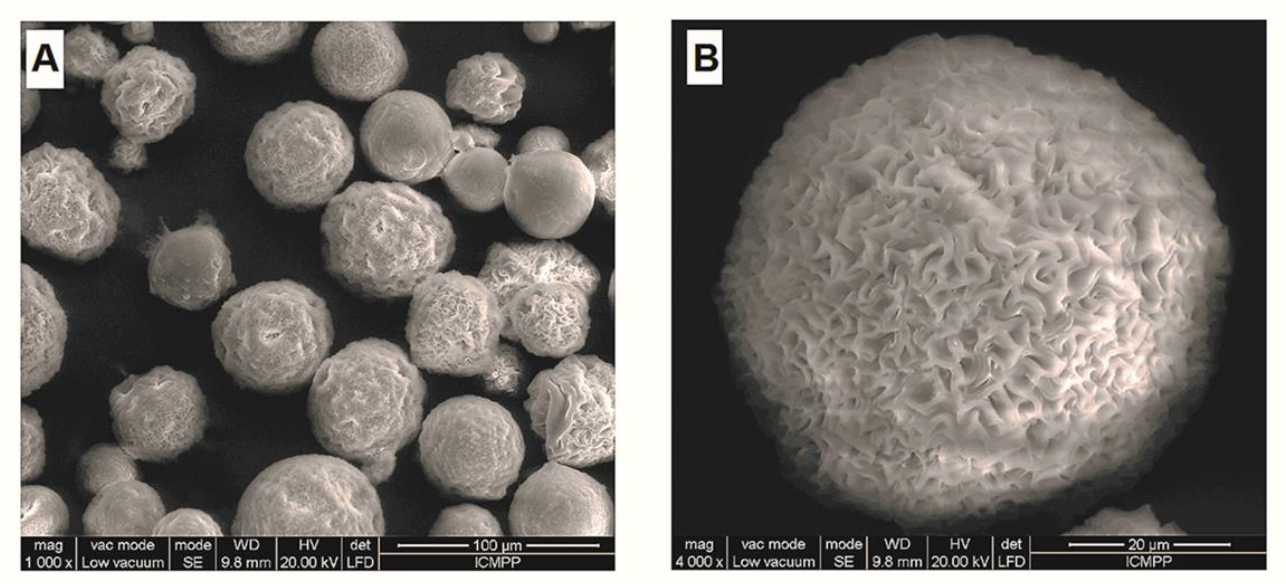


**Fig. 1.** Scanning electron micrographs of dried CS microspheres: general view (panel A), and surface detail (panel B).

### *3.2. Preparation of hydrogels loaded with CS microspheres*

Smart composite hydrogels containing CS microspheres were prepared by free radical polymerization of NIPAAm and HEAAm in the presence of BisAAm as cross-linker and APS and TEMED as initiator system (Fig. 2A).

Fundueanu et al. (2013) found that the linear copolymer P(NIPAAm-co-HEAAm) obtained at 10:2 molar ratio of the co-monomers in the initial reaction mixture, has a lower critical solution temperature (LCST) value close to that of the body temperature (37.6 $^{o}$C in simulated intestinal fluid). Consequently, we used this composition of co-monomers for the hydrogels synthesis, with or without CS microspheres incorporated. The composition of the reaction mixture as well as the composition of the final smart hydrogel is given in Table 1.

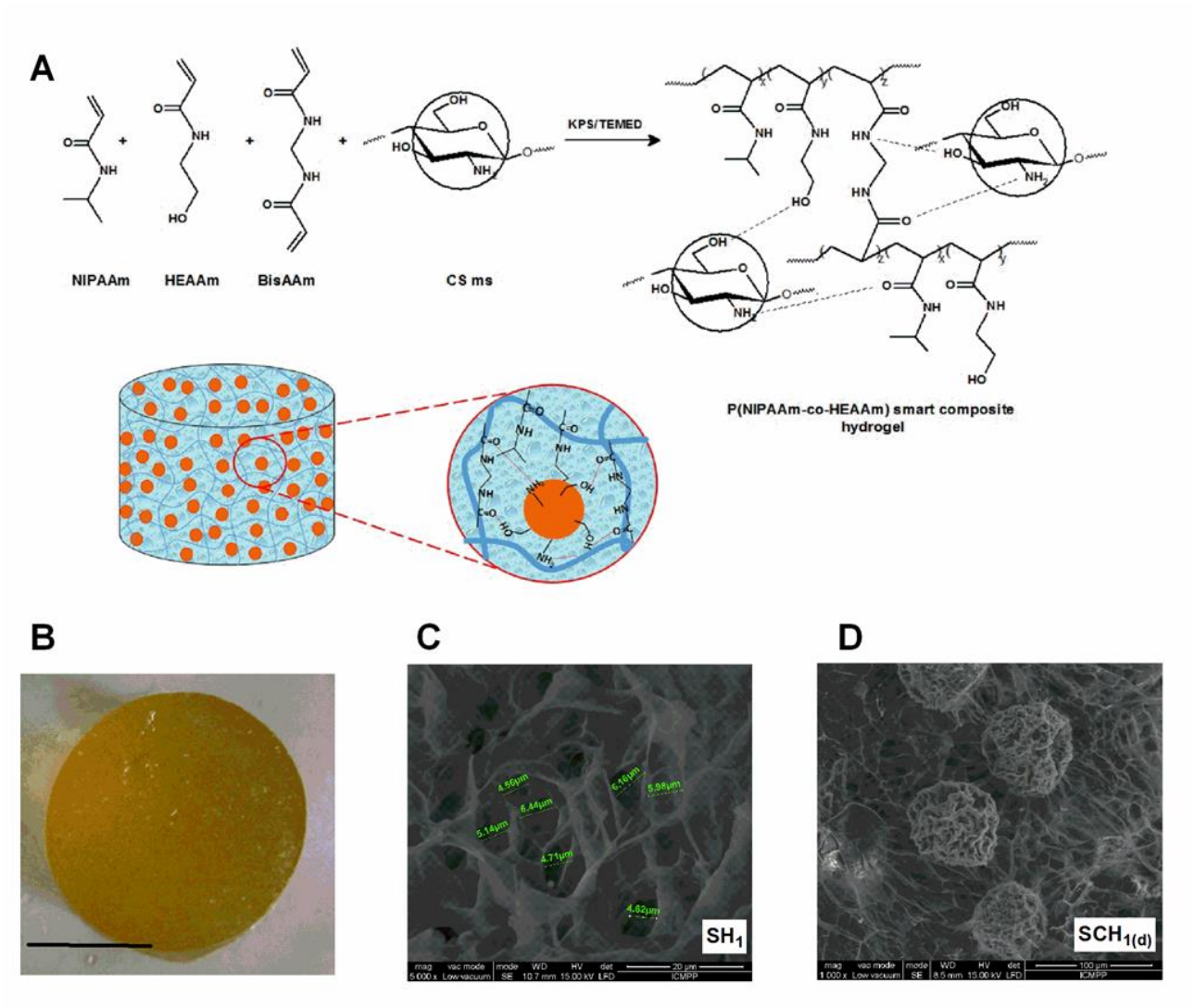


**Fig. 2.** Schematic representation of the synthesis steps of smart composite hydrogels (panel A). Optical photomicrograph of swollen smart composite hydrogels ($SCH_{1(d)}$) in water at 23 ºC (panel B). The bar corresponds to 1 cm. Scanning electron micrographs of freeze-dried smart ($SH_1$) (panel C) and smart composite hydrogels ($SCH_{1(d)}$) (panel D).

**Table 1.** Feed compositions and final characteristics of smart and smart composite hydrogels

| | $SH_{0.5}$ | $SH_1$ | $SH_2$ | $SCH_{0.5}$ | $SCH_1$ | $SCH_2$ | $SCH_{1(d)}$ |
|---|---|---|---|---|---|---|---|
| NIPAAm (mg) | 700 | 700 | 700 | 700 | 700 | 700 | 700 |
| HEAAm (mg) | 150 | 150 | 150 | 150 | 150 | 150 | 150 |
| CS ms (mg) | - | - | - | 150 | 150 | 150 | 300 |
| $H_2O$ (ml) | 10 | 10 | 10 | 10 | 10 | 10 | 10 |
| BisAAm (mg) | 4.25 | 8.5 | 17 | 4.25 | 8.5 | 17 | 8.5 |
| KPS (mg) | 25.5 | 25.5 | 25.5 | 25.5 | 25.5 | 25.5 | 25.5 |
| TEMED (μL) | 40 | 40 | 40 | 40 | 40 | 40 | 40 |
| CS ms in SCH (mg/g)[a] | - | - | - | 119 ± 10 | 107 ± 11 | 110 ± 13 | 261 ± 22* |
| $SA_a$ content (mg/g)[b] | - | - | - | 52.4 ± 5.0 | 44.4 ± 4.9 | 46.8 ± 5.2 | 115.4 ± 11.1* |
| $SA_t$ content (mg/g)[c] | - | - | - | 60.7 ± 5.1 | 54.6 ± 5.6 | 56.2 ± 6.6 | 133.3 ± 11* |
| SA loading efficiency (%) | - | - | - | 86.2 ± 8.2 | 81.3 ± 8.9 | 83.3 ± 9.3 | 86.6 ± 8.3 |

[a]The amount of CS microspheres in SCH was determined by conductometric titration of amine groups with 0.1 M NaOH solution.
[b]$SA_a$ content is expressed as the amount of SA per 1g of dried SCH
[c]$SA_t$ content is determined taking into account the exchange capacity of CS microspheres
*statistically significant differences

### *3.3. Shape and morphology of SCH hydrogels*

Optical image of $SCH_{1(d)}$ are shown in Fig. 2B. It is obvious that yellow CS micospheres are present in the transparent P(NIPAAm-co-HEAAm) hydrogel and they are uniform enough distributed in the polymeric network. SCHs were relatively stable, no visual difference being observed even after immersion in water for 21 days.

The interior morphology of SHs and SCHs is shown in Fig. 2C. Microspheres were distributed regularly in all hydrogels. It can be noticed that CS microspheres are incorporated into the hydrogel network and not in its pores, and the network porosity around the microspheres slightly increases.

### *3.4. Temperature and pH responsive properties*

Since SCHs were designed for biomedical applications, their temperature and pH responsive properties were studied in simulated physiological fluids (standard acid solution of pH 1.2 and phosphate buffer of pH 7.4).

#### *3.4.1. VPTT*

The VPTT of SCHs was examined by measuring the temperature dependence of the equilibrium swelling ratio. VPTT was determined as the value of the inflection point from the curve representing the variation of degree of swelling *versus* temperature.

Fig. 3 shows the temperature-dependent swelling ratios over a temperature range from 23 to 60 $^{o}$C. All SCHs presented a similar temperature dependence of the equilibrium swelling ratios, i.e., the swelling ratio decreased quickly as the temperature increased. The VPTT of the samples was determined by the inflection point of the Boltzmann sigmoid equation fit of the data, and was approximately 34.5 ± 0.2 $^{o}$C at pH 1.2 and 33.1 ± 0.3 $^{o}$C at pH 7.4, irrespective of the microspheres amount in SCHs.

Swelling ratios, as well as the sharpness of the phase transitions, largely depend on the cross-linking degree. Thus, with increasing the amount of BisAAm, swelling ratios decreased significantly, especially at temperatures situated below the VPTT. In this temperature range, interactions between water and polymer chains prevail leading to high degrees of swelling. Also, below the VPTT, swelling ratios in PBS (pH 7.4) are lower than in acidic pH (pH 1.2). In fact, at pH 7.4, the free amino groups of CS are not ionized ($pK_a$ = 6.5) (Goycoolea et al., 2003) and therefore can form hydrogen bonds with the amide or hydroxyl groups from P(NIPAAm-co-HEAAm) network, reducing the mobility of the polymer chains. On the contrary, in acidic pH (pH 1.2), the amino groups of chitosan are in protonated state, and therefore they are not able to form hydrogen bonds with the polymeric network. Moreover, in the protonated state, CS micropsheres are more hydrophilic, and thus more expanded. With the increasing of temperature above the VPTT, hydrogels collapsed and the differences between swelling ratios are greatly reduced in both

simulated physiological solutions, despite the amount of cross-linker used. Above the VPTT, the hydrophobic interactions between polymer chains are countered by the presence of the hydrophilic CS microspheres. However, the hydrophobic interactions predominate and the SCHs collapsed.

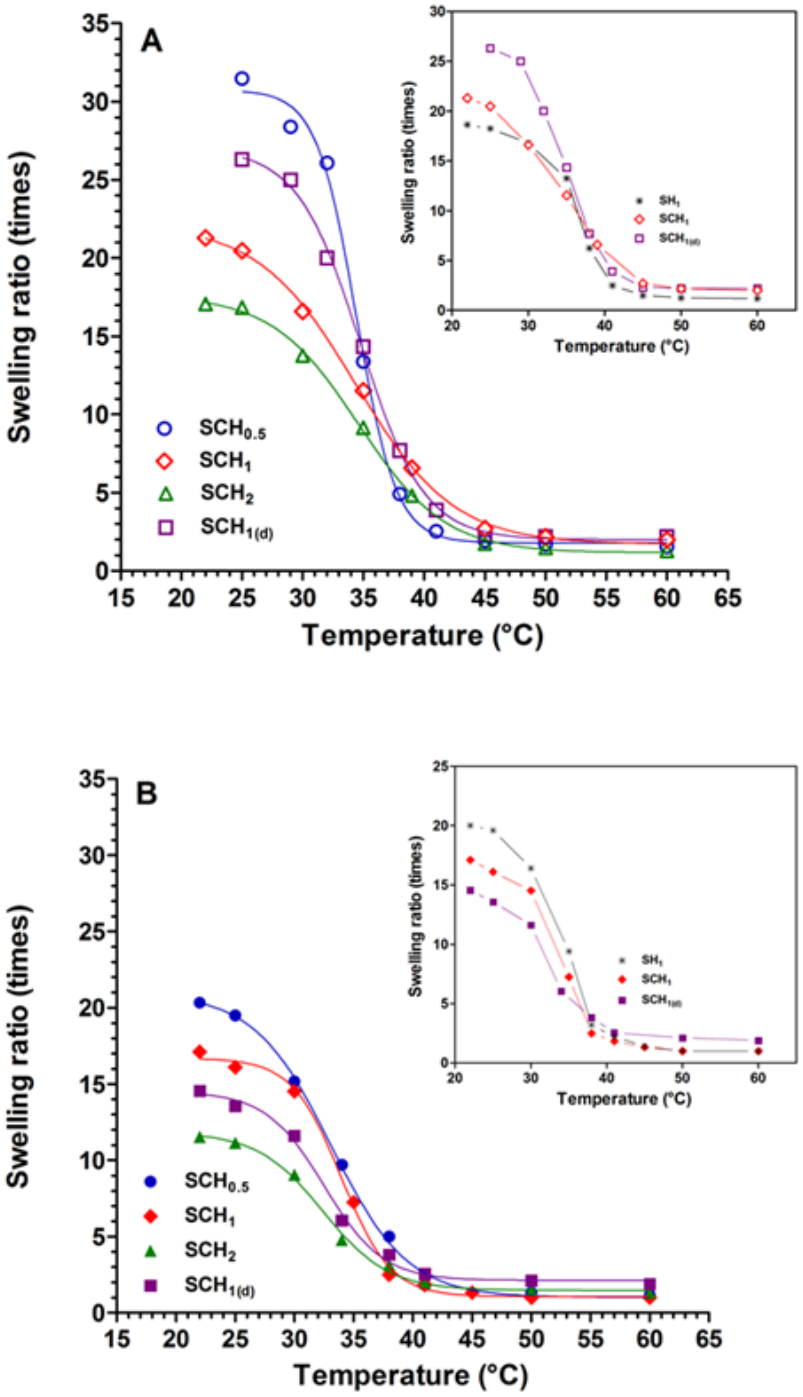


**Fig. 3.** Equillibrium swelling ratios of composite hydrogels in simulated physiological fluids: standard acid solution with pH 1.2 (panel A) and phosphate buffer solution with pH 7.4 (panel B). The curves are Boltzmann sigmoid equation fits of the data.

All these observations are sustained by the difference between the swelling ratios of SH and SCHs in both simulating conditions (Fig. 3A,B; inset). It is obvious that the presence of CS microspheres in SCHs determines the swelling ratio values at temperatures situated below the VPTT. These values are either higher or lower than those of simple hydrogels based on the ionization state of CS microspheres in simulated physiological fluids.

### *3.4.2. Swelling kinetics*

Swelling rate is an important characteristic of the composite hydrogels sensitive to both pH and temperature, designed to be used in the controlled release of bioactive compounds. Therefore, the swelling kinetics of SCHs were investigated in relation with temperature, pH, cross-linking degree, and the amount of embedded CS microspheres.

Fig. 4 shows the swelling kinetics of SCHs at 23 $^{o}$C (under VPTT) in PBS at pH 7.4 (panel A) and standard acidic solution at pH 1.2 (panel B). As a general rule, all composite hydrogels showed higher swelling rates in acidic than in basic pH. As previously mentioned, the pH sensitivity is induced by chitosan microspheres. Thus, the equilibrium swelling ratio of $SCH_{0.5}$ at 24 h, in acidic solution, are ~25 % higher than in PBS; this value increases to ~60% for $SCH_{1(d)}$. In fact, at pH 1.2, the amine groups of chitosan microspheres are in the protonated state favoring the swelling of the microspheres, and finally resulting in an expansion of the network. This theory is also supported by comparing the swelling kinetics of $SCH_{1(d)}$ and $SCH_1$ samples. The maximum swelling ratio increased with about 1.2 times when the amount of entrapped microspheres are double, due to the network expansion (forcing cross-linking bridges by the high density of the microspheres).

Graphs presented in Fig. 4 also indicate that the key factor influencing the swelling kinetics is the cross-linking degree. It is evident that the swelling rate decreases with the increase of the amount of cross-linker. A highly cross-linked network displays a reduced mobility of the polymer chains and therefore a lower swelling rate. For example, the hydrogel obtained with 2% BisAAm ($SCH_2$) showed the lowest swelling rate due to a more compact structure. On the opposite, the sample obtained with

0.5 % BisAAm ($SCH_{0.5}$) displays the highest swelling rate, irrespective of pH (Fig. 4A,B). It must be noticed that in PBS at pH 7.4 the swelling rate can be reduced by the hydrogen bonds formed between the amine groups of chitosan microspheres and hydroxyl groups of HEAAm or amide groups of the thermo-sensitive component of hydrogel (NIPAAm).

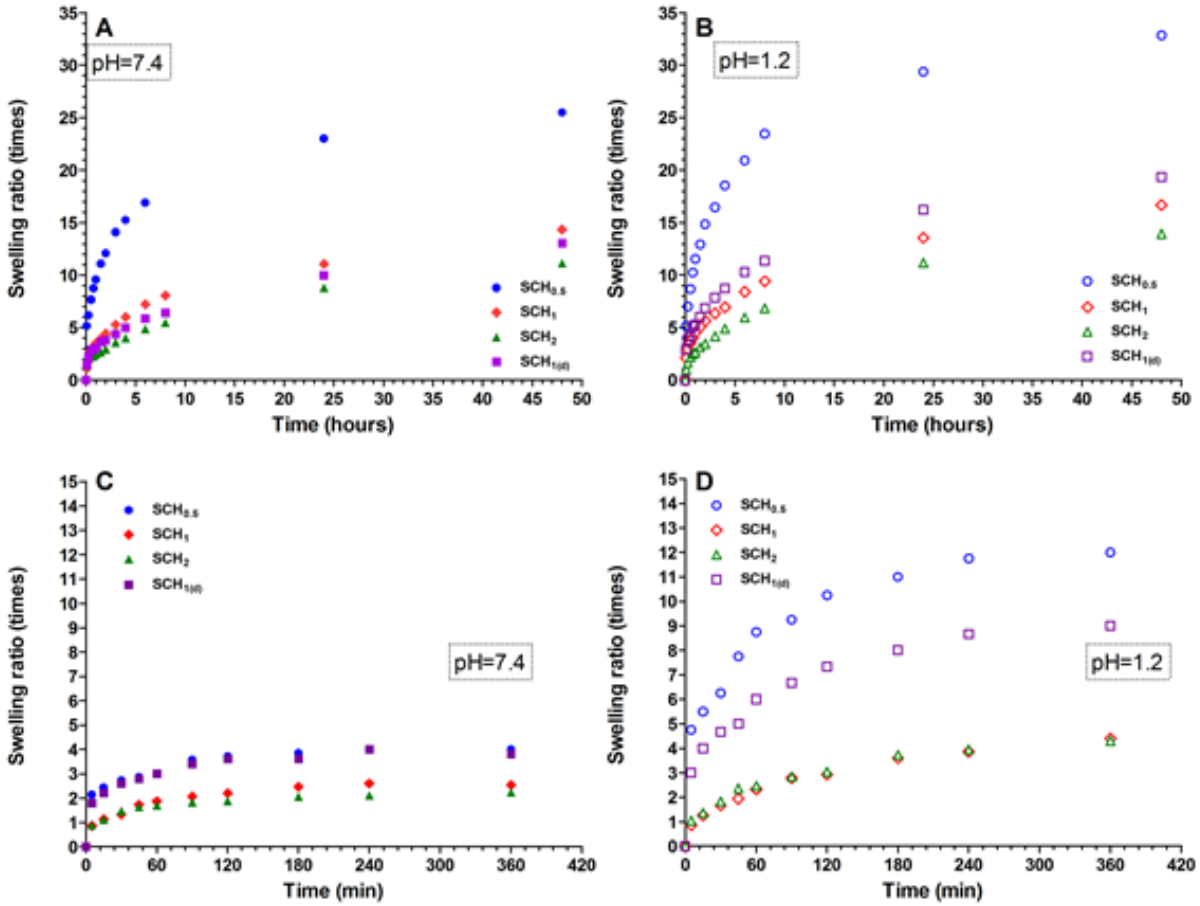


**Fig. 4.** Swelling kinetic curves of smart composite hydrogels at 23 ºC (panels A and B) and 37 ºC (panels C and D) in phosphate buffer solution at pH 7.4 and in standard acidic solution at pH 1.2.

At a temperature situated above the VPTT (37 °C), the equilibrium swelling ratios of the composite hydrogels are noticeably more decreased (Fig. 4C,D) than at 23 °C (Fig. 4A,B). Swelling occurs rapidly in the first minutes after which the rate of swelling increases slowly in the next few hours until reaching equilibrium.

Loss of swelling is due to the partial disruption of hydrogen bonds between the water molecules and the amide groups of PNIPAAm and the occurrence, during the phase transition, of hydrogen

bondings, intra- and inter-molecular between C=O and NH. In addition, the dehydrated polymeric chains interact hydrophobically, resulting a compact structure with a low swelling capacity.

With respect to the equilibrium, this is achieved much faster at 37 °C (near VPTT) than at 23 °C. For example, at 37 °C, the most swellable smart hydrogel ($SCH_{0.5}$) reached equilibrium after 4 hours at pH 7.4 (Fig. 4C) and 6 hours at pH 1.2 (Fig. 4D). On the opposite, at 23 °C, the same sample reached equilibrium after 48 hours both in PBS and acidic solution at pH 1.2. In PBS, the swelling ratio of $SCH_{0.5}$ after 6 hours at room temperature (Fig. 4A) is about 4 times higher than at 37 °C (Fig. 4C).

### *3.4.3. Swelling/deswelling kinetics*

One of the major requirements of the smart hydrogels used in biomedical applications is to display fast swelling/collapsing rates whenever small temperature change occurred. It is well-known that the rapidity of the swelling and collapsing processes of a thermosensitive hydrogel depends to the diffusion rate of water to/from hydrogel. The diffusion rate is controlled mainly by the size and the porosity of the hydrogel (Tanaka & Fillmore, 1979; Wu, Hoffman & Yager, 1992). Obviously, hydrogels with small dimensions and high porosity allow a fast diffusion of water in/out and therefore display high swelling/deswelling rates. SCHs synthesized in this study exhibit a very porous structure; however the dimensions of each sample are large enough (15 mm in diameter and 10 mm in thickness). As follows, the swelling/deswelling rates of SCHs were moderate both in PBS at pH 7.4 and in acidic solution at pH 1.2. (Fig. 5A,B). Also, it can be observed that the swelling/deswelling of SCHs is a reversible process being in agreement with the temperature changes. As expected, SCHs with the lowest BisAAm content ($SCH_{0.5}$) or with the largest amount of entrapped CS microspheres ($SCH_{1(d)}$) have the highest difference of the swelling ratios when the temperature changes from below to above the VPTT or vice versa. It can be also noticed that the collapsing rate is higher than the swelling one because the buffer is ejected mechanically during the collapse of hydrogel.

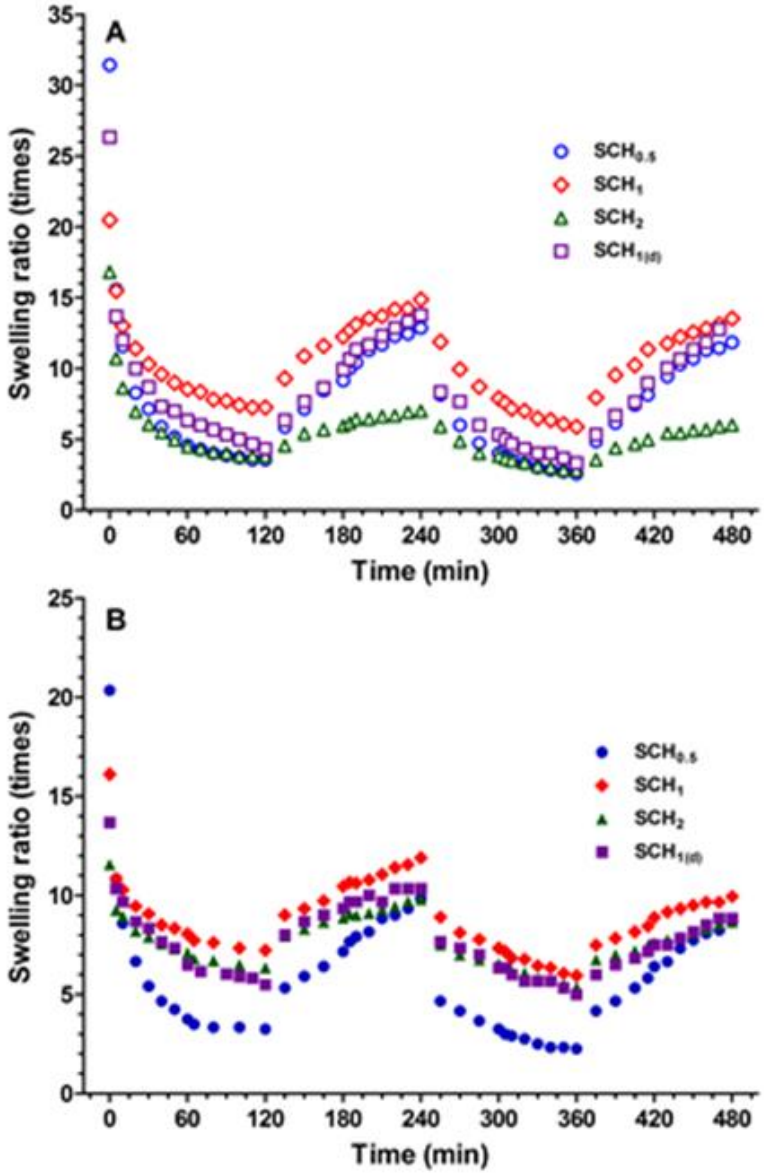


**Fig. 5.** Pulsatile temperature-dependent swelling behaviour of SCHs in response to temperature changes between 23 and 42 $^{o}$C, recorded in acidic solution at pH 1.2 (panel A) and phosphate buffer solution at pH 7.4 (panel B).

### *3.5. In vitro degradation studies*

The change of the mass for both CS microspheres and $SCH_1$ is shown in Fig. 6. During 4 weeks degradation experiment, the weight losses of CS microspheres were 13.05 % and 28.4 % in PBS, in the absence and in the presence of lysozyme, respectively (Fig. 6A). Assuming that only CS microspheres from P(NIPAAm-co-HEAAm) hydrogel degrades with the same rate as free

microspheres, the theoretical mass loss of $SCH_1$ should be 1.4 % and 3.04 % in PBS without and with lyzozyme, respectively. However, the actual values are lower (1.2 % and 2.6 %) (Fig. 6B). Probably, at the body temperature (37 $^{o}$C), the polymeric network maintains a hydrophobic microclimate around the CS microspheres reducing the degradation rate. Moreover, the activity of lysozyme can be obstructed in such a network. In PBS, the dry weight remaining ratio of CS microspheres decreased from 100 % to 86.95 %, while the dry $SCH_1$ remaining ratio remained unchanged during the first 3 days, and then slowly decreased reaching 98.8 % at the end of the experiment. In 1 mg/mL lysozyme/PBS solution, the weight remaining ratio of CS microspheres constantly decreased until 71.60 % in 28 days of immersion, due to the CS degradability accelerated in the presence of lysozyme.

Comparing the four types of smart hydrogels at the same time point (Fig. 6C), the higher cross-linked hydrogel ($SCH_2$) showed less weight loss than the others due to his lower swelling degree in the degradation environment. However, the weight loss of the SCHs composites increases with the enhancement of CS microspheres amount ($SCH_{1(d)}$), indicating that hydrophilic CS with a large specific area can facilitate the infiltration of water inside of SCH structure resulting in an enhanced degradation of SCHs composites.

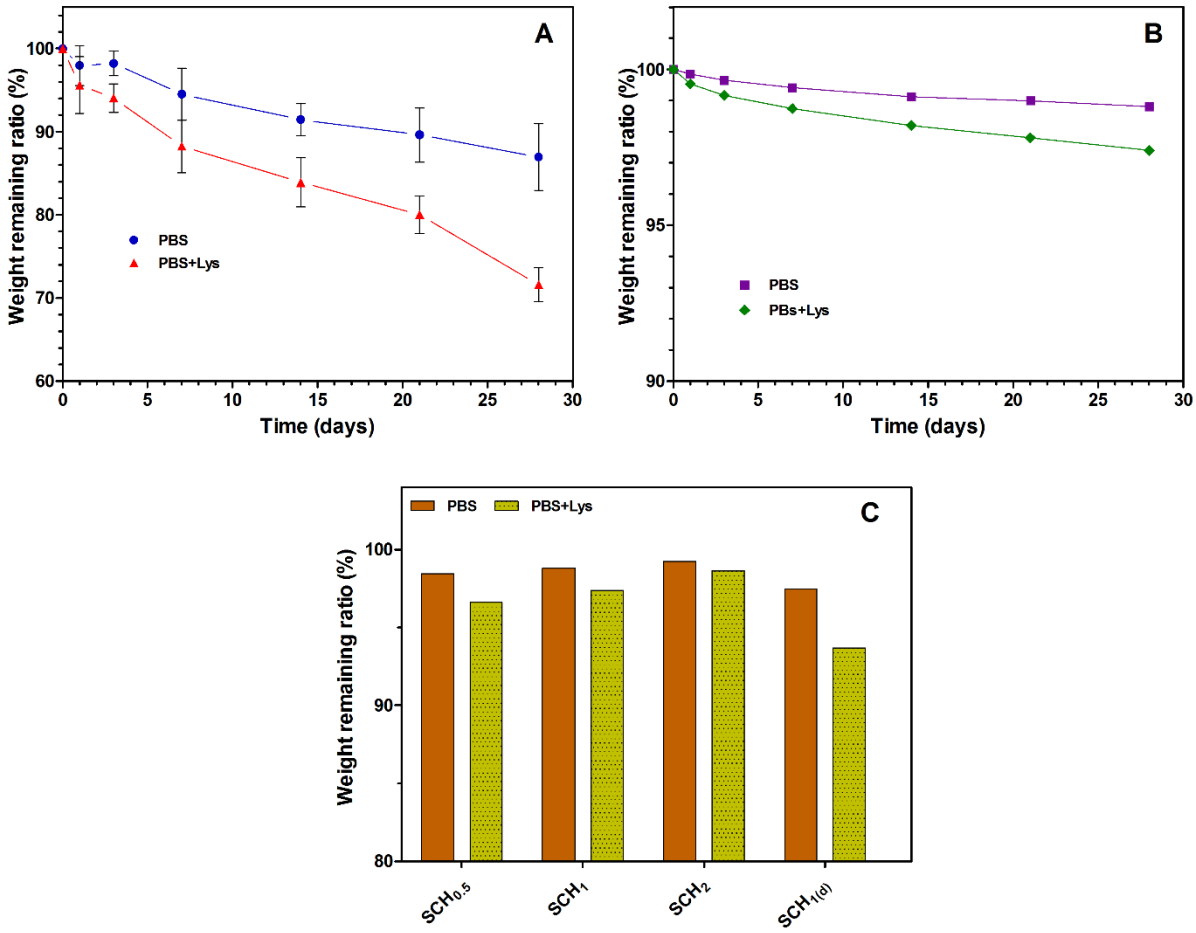


**Fig. 6.** Weight remaining ratio *vs* degradation time for CS microspheres (panel A) and $SCH_1$ (panel B). Weight remaining ratio at 4 weeks for SCHs (panel C).

The change in the structure of the chitosan microspheres during the degradation was observed by SEM and compared with that of SCHs (Fig. 7). No visible change of the surface morphology was observed from day 1 to day 28 in PBS for CS microspheres (Fig. 7A). After 7 days of degradation in lysozyme/PBS solution, the microspheres surface become smoother while after 28 days, cracks are seen on the surface and a start of the lost their spherical structure (Fig. 7B).

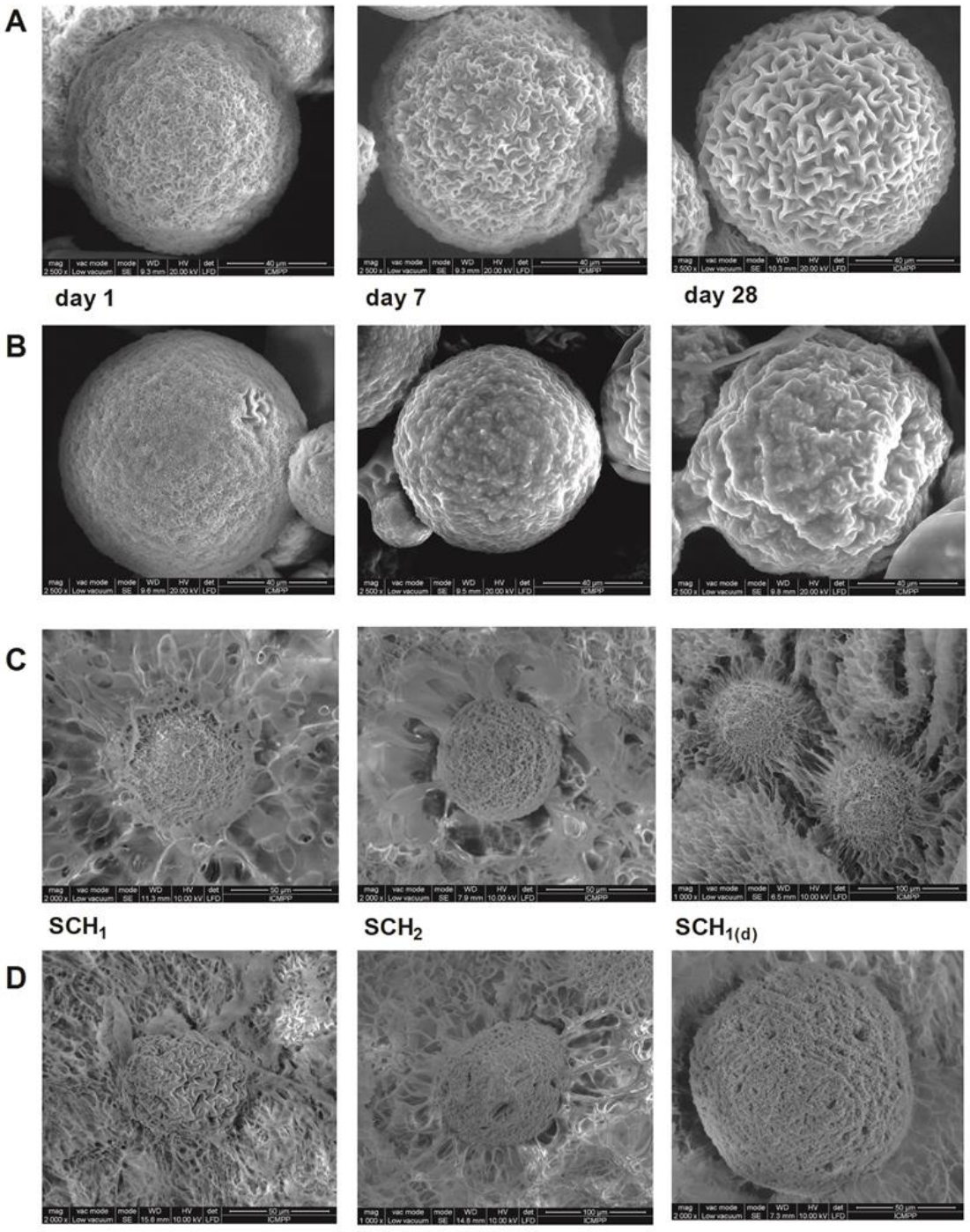


**Fig. 7.** Scaning electron micrographs of CS microspheres after 1, 7 and 28 days of degradation in phosphate buffer solution (panel A) and 1 mg/mL lysozyme/phosphate buffer solution (panel B). Scanning electron micrographs of SCHs after 28 days of degradation in phosphate buffer solution (panel C) and 1 mg/mL lysozyme/phosphate buffer solution (panel D).

In the case of SCHs (Fig. 7D), the network pores are collapsed together after degradation for 4 weeks in lysozyme/PBS solution. This could be due to that degradation reduces the mechanical strength more or less, leading to a larger extent of collapse of the hydrogel upon drying.

After 4 weeks of degradation in PBS, some pores are observed on the microspheres surface embedded in $SCH_{1(d)}$ hydrogel (Fig. 7C). At the same point, but in 1 mg/mL lysozyme/PBS solution, microspheres embedded in $SCH_2$ and $SCH_{1(d)}$ showed more pores on the surface or a more folded surface in the case of $SCH_1$. These observations are consistent with the results shown in Fig. 6B,C.

***In vitro release studies***

The drug release from the pH/thermoresponsive SCHs is governed on the one hand by the temperature and pH which modulates the swelling degree of the network. On the other hand, since SA is electrostatically linked to CS microspheres, the release of the drug should be firstly controlled by the breaking rate of the electrostatic bonds and secondly by diffusion through the polymeric network. The diffusion of SA from SCHs to the release medium will be controlled by steric interactions between drug and the polymer network.

The release kinetics of SA from CS microspheres and SCHs in PBS at pH 7.4 and acidic solution at pH 1.2, at different temperatures (23, 37, and 42 $^{o}$C) are presented in Fig. 8.

In PBS at 37 $^{o}$C (Fig. 8A) the drug is rapidly released from the CS microspheres with a 86 % initial release in the first 5 minutes. Therefore, the electrostatic interactions between carboxylic groups of SA and amino groups of CS as well as the diffusion through the polymeric network of CS do not influence the release rate. Compared with the fast release profiles from the CS microspheres, the release kinetics of SA from SCHs exhibits a delayed release pattern which lasted 24 hours and more. SA release profiles follow the swelling pattern, with a time to show a maximum of 80 % release being 6 h for $SCH_{0.5}$, and 24 h for $SCH_1$ and $SCH_2$. SA was released in a ~ 90 % from $SCH_{1(d)}$ after 24 hours of immersion.

The SA release profiles in simulated gastrointestinal conditions (2 hours at pH 1.2 followed by 22 hours at pH 7.4) from $SCH_1$ sample is shown in Fig. 8B. The amount of released SA is low in the first 2 hours despite the fact that the swelling ratio is higher at this pH. In fact, in acidic conditions, SA is in protonated state, less soluble. The pH change of the release medium from 1.2 to 7.4 has two opposite effects: the increase of the drug solubility and the decrease of the swelling ratio of CS microspheres. Therefore, an initial large amount of SA is released in the first minutes followed by a delayed released over a large period of time.

The influence of temperature on SA release kinetics in PBS, from $SCH_1$ sample, is displayed in Fig. 8C. Below VPTT (23 $^oC$), the SA is quickly released in PBS at pH 7.4, since the SCH is in the swollen state and no steric interactions occur. When the temperature was raised above VPTT (37 and 42 $^oC$), the polymeric network was dehydrated, became hydrophobic and collapsed. Moreover, an increased temperature favorized hydrophobic interactions between SA and thermosensitive hydrogel. Therefore, the release rate should be substantially reduced. On the contrary, a high temperature increased the solubility and the diffusion rate of drug. As a result of these contrary effects, the release rate of SA is low at temperatures situated above VPTT. The lowest release rate was recorded at 42 $^oC$, when the polymeric network is completely collapsed (see Fig. 3, panel B). Fig. 8D shows the SA release profile from $SCH_1$ hydrogel as a function of temperature cycling at fixed pH value (PBS pH 7.4). The pulsatile release followed a two stages pattern. The initial release comprises of the first 3 thermal cycles (up until 3.5 hours) and unexpected, the SA amount released at elevated temperature is higher than at low temperature. In fact, the change of the temperature every 30 minutes does not allow a complete swelling/collapse of the hydrogel, processes requiring at least 2 hours (see Fig. 5B). In this case, there is a burst release (802 and 853 μg/30 min release rate) during the $1^{st}$ and $2^{nd}$ temperature cycles, respectively. The amounts of SA released in the subsequently thermal cycles are lower and lower, i.e. release rates drop down continuous to a range of 205—311 μg/30 min at 42 $^oC$ and 80-127 μg/30 min at 23 $^oC$.

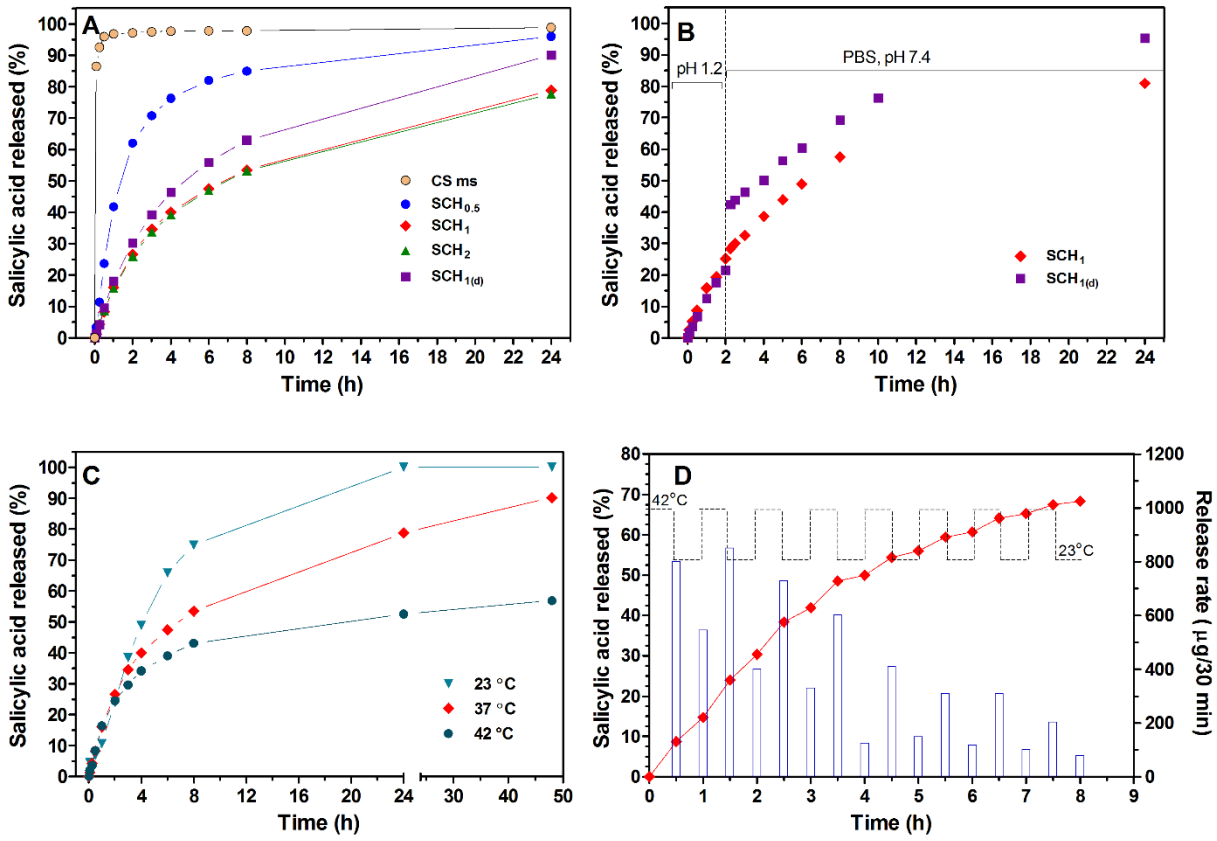


**Fig. 8.** Release patterns of SA from SCHs in standard phosphate buffer solution of pH 7.4 at 37 ºC (panel A). For comparison, it is depicted the release profile of SA from CS microspheres. Release profiles of SA from $SCH_1$ in simulated gastro-intestinal conditions at 37 ºC (panel B), in phosphate buffer solution of pH 7.4 at different temperatures (panel C), and under thermal cycling conditions (panel D).

## Conclusions

CS microspheres were prepared taking into account their remarkable properties: high capacity to load opposite charged molecules, such as SA, pH-sensitivity and biodegradability. However, due to the presence of competitive ions in the physiological fluids, the drug has been rapidly displaced and released. Therefore, to reduce the release rate as well as to confer sensitivity to temperature, the microspheres were embedded within a thermosensitive hydrogel based on P(NIPAAm-co-HEAAm), resulting a smart composite hydrogel (SCH). The morphology, swelling degree and

swelling kinetics of SCH depend to the pH and temperature as well as the cross-linking degree. Compared with the fast release rate from the CS microspheres, the release kinetics of SA from SCH exhibit a delayed release pattern which lasted 24 hours and more. Moreover, the release rate strongly depends to pH and temperature. The thermoresponsive network has been shown to have a weak protection against *in vitro* CS microspheres degradation.

**Acknowledgements**

The authors are grateful for the financial support from the H2020 ERA Chairs Project no 667387: SupraChem Lab Laboratory of Supramolecular Chemistry for Adaptive Delivery Systems ERA Chair initiative.

## References

Amin, S., Rajabnezhad, S., & Kohli, K. (2009). Hydrogels as potential drug delivery systems. *Scientific Research and Essay, 3,* 1175-1183.

Bae, Y. H. (1997). Stimuli-Sensitive Drug Delivery. In: K. Park (Ed.), *Controlled Drug Delivery: Challenge and Strategies* (pp.147–160). Washington, DC: American Chemical Society.

Bae, Y. H., Okano, T., Hsu, R., & Kim, S. W. (1987). Thermosensitive polymers as on–off switches for drug release. *Die Makromolekulare Chemie, Rapid Communications, 8,* 481–485.

Bae, Y. H., Okano, T., & Kim, S. W. (1990).Temperature dependence of swelling of crosslinked poly(N,N'-alkyl substituted acrylamides) in water. *Journal of Polymer Science Part B: Polymer Physics, 28,* 923–936.

Bajpai, S. K., & Sonkusley, J. (2002). Hydrogels for oral drug delivery of peptides: Synthesis and characterization. *Journal of Applied Polymer Science, 83,* 1717-1729.

Bromberg, L. E., & Ron, E. S. (1998). Temperature-responsive gels and thermogelling polymer matrices for protein and peptide delivery. *Advanced Drug Delivery Reviews, 31,* 197–221.

Cai, D. -Z., Zheng, C., Quan, D. -P., Bu, L. S., Wang, K., Lu, H. -D., & Li, X. -F. (2007). Biodegradable chitosan scaffolds containing microspheres as carriers for controlled transforming growth factor-beta1 delivery for cartilage tissue engineering. *Chinese Medical Journal, 120,* 197-203.

Dash, M., Federica, C., Ottenbrite, R., & Chiellini, E. (2011). Chitosan-a versatile semi-synthetic polymer in biomedical applications. *Progress in Polymer Science, 36,* 981-1014.

De Alvarenga, E. S., de Oliveira, C. P., & Bellato, C. R. (2010). An approach to understanding the deacetylation degree of chitosan. *Carbohydrate Polymers, 80,* 1155–1160.

El-Leithy, E. S., Shaker, D. S., Ghorab, M. K., & Abdel-Rashid, R. S. (2010). Evaluation of mucoadhesive hydrogels loaded with diclofenac sodium-chitosan microspheres for rectal administration. *AAPS PharmSciTech, 11,* 1695-1702.

Fundueanu, G., Constantin, M., Asmarandei, I., Bucatariu, S., Harabagiu, V., Ascenzi, P., & Simionescu, B. C. (2013). Poly(N-isopropylacrylamide-co-hydroxyethylacrylamide) thermosensitive microspheres: The size of microgels dictates the pulsatile release mechanism. *European Journal of Pharmaceutics, 85,* 614-623.

Fundueanu, G., Constantin, M., Bortolotti, F., Ascenzi, P., Cortesi, R., & Menegatti, E. (2005). Preparation and characterisation of thermoresponsive poly(Nisopropylacrylamide-co-acrylamide-co-hydroxyethyl acrylate) microspheres as a matrix for the pulsed release of drugs. *Macromolecular Bioscience, 5,* 955–964.

Gandhi, A., Paul, A., Sen, S. O., & Sen, K. K. (2015). Studies on thermoresponsive polymers: Phase behaviour, drug delivery and biomedical applications. *Asian Journal of Pharmaceutical Sciences, 10,* 99-107.

Goycoolea, F. M., Heras, A., Aranaz, I., Galed, G., Fernández-Valle, M. E., & Argüelles-Monal, W. (2003). Effect of Chemical Crosslinking on the Swelling and Shrinking Properties of Thermal and pH-Responsive Chitosan Hydrogels. *Macromolecular Bioscience, 3,* 612-619.

Graham, N. B., & Mc-Neil, M. E. (1984). Hydrogels for controlled drug delivery. *Biomaterials, 5,* 27-36.

Grinberg, V. Y., Dubovik, A. S., Kuznetsov, D. V., Grinberg, N. V., Grosberg, A. Y., & Tanaka, T. (2000). Studies of the thermal volume transition of poly(N-isopropylacrylamide) hydrogels by high-sensitivity differential scanning microcalorimetry. 2. Thermodynamic functions. *Macromolecules, 33,* 8685–8692.

Hoffman, A. S. (1997). Intelligent Polymers. In: K. Park (Ed.), *Controlled Drug Delivery: Challenge and Strategies* (pp. 485–497). Washington, DC: American Chemical Society.

Hoffman, A. S., Afrassiabi, A., & Dong, L. C. (1986). Thermally reversible hydrogels. II. Delivery and selective removal of substances from aqueous solutions. *Journal of Controlled Release, 4,* 213–22.

Illum, L. (1998). Chitosan and its use as a pharmaceutical excipient. *Pharmaceutical Research, 15,* 1326–1331.

Illum, L., Jabbal-Gill, I., Hinchcliffe, M., Fisher, A. N., & Davis, S. S. (2001). Chitosan as a novel nasal delivery system for vaccines. *Advanced Drug Delivery Reviews, 51,* 81-96.

Inomata, H., Wada, N., Yagi, Y., Goto, S., & Saito, S. (1995). Swelling behaviors of N-alkylacrylamide gels in water: effects of copolymerization and crosslinking density. *Polymer, 36,* 875–877.

Joung, Y. K., Choi, J. H., Park, K. M., & Park, K. D. (2007). PLGA microparticle-embedded thermosensitive hydrogels for sustained release of hydrophobic drugs. *Biomedical Materials, 2,* 269-273.

Kamath, K., & Park, K. (1993). Biodegradable hydrogels in drug delivery. *Advanced Drug Delivery Reviews, 11,* 85-108.

Lin, Y., Sun, J., Jiang, G., Zan, J., & Ding, F. (2007). In vitro Evaluation of Lysozyme-Loaded Microspheres in Thermosensitive Methylcellulose-Based Hydrogel. *Chinese Journal of Chemical Engineering, 15,* 566-572.

Liu, W. -F., Kang, C. -Z., Kong, M., Li, Y., Yi, A., Cheng, X. -J., & Chen, X. -G. (2012). Controlled release behaviors of chitosan/α,β-glycerophosphate thermo-sensitive hydrogels. *Frontiers of Materials Science, 6,* 250-258.

Majeti, N. V., & Ravi, K. (2000). A review of chitin and chitosan applications. *Reactive and Functional Polymers, 46,* 1-27.

Mengatto, L. N., Helbling, I. M., & Luna, J. A. (2012). Recent Advances in Chitosan Films for Controlled Release of Drugs. *Recent Patents on Drug Delivery & Formulation, 6,* 156-170.

Mitra, A., & Dey, B. (2011). Chitosan Microspheres in Novel Drug Delivery Systems. *Indian Journal of Pharmaceutical Sciences, 73,* 355-366.

Morris, G. A., Kök, M. S., Harding, S. E., & Adams, G. G. (2010). Polysaccharide drug delivery systems based on pectin and chitosan. *Biotechnology and Genetic Engineering Reviews, 27,* 257-284.

Ngah, W. S. W., Endud, C. S., & Mayanar, R. (2002). Removal of copper(II) ions from aqueous solution onto chitosan and cross-linked chitosan beads. *Reactive and Functional Polymers, 50,* 181–190.

Niu, X., Feng, Q., Wang, M., Guo, X., & Zheng, Q. (2009). In vitro degradation and release behavior of porous poly(lactic acid) scaffolds containing chitosan microspheres as a carrier for BMP-2-derived synthetic peptide. *Polymer Degradation and Stability, 94,* 176-182.

Park, K., & Park, H. (1999). Smart Hydrogels. In: J.C. Salamone (Ed.), *Concise Polymeric Materials Encyclopedia* (pp. 1476–1478). Boca Raton: CRC Press.

Park, K., Shalaby, W. S. W., & Park, H. (1993). *Biodegradable Hydrogels For Drug Delivery*. Lancaster, Technomic.

Tanaka, T., & Fillmore, D. J. (1979). Kinetics of swelling of gels. *The Journal of Chemical Physics, 70,* 1214–1218.

Tang, Y., Zhao, Y., Li, Y., & Du, Y. (2010). A thermosensitive chitosan/poly(vinyl alcohol) hydrogel containing nanoparticles for drug delivery. *Polymer Bulletin, 64,* 791-804.

Wu, X. S., Hoffman, A. S., & Yager, P. (1992). Synthesis and characterization of thermally reversible macroporous poly(N-isopropylacrylamide) hydrogels. *Journal of Polymer Science Part A: Polymer Chemistry, 30*, 2121–2129.

Zhang, X. Z., Wu, D. Q., & Chu, C. C. (2004). Synthesis, characterization and controlled drug release of thermosensitive IPN–PNIPAAm hydrogels. *Biomaterials, 25*, 3793–3805.

Zhang, X. Z., Zhuo, R. X., Cui, J. Z., & Zhang, J. T. (2002). A novel thermoresponsive drug delivery system with positive controlled release. *International Journal of Pharmaceutics, 235*, 43–50.